THE JOURNAL OF BIOLOGICAL CHEMISTRY Vol. 280, No. 25, Issue of June 24, pp. 23900–23909, 2005

Printed in U.S.A.

High Resolution Structures of Highly Bulged Viral Epitopes Bound to Major Histocompatibility Complex Class I

IMPLICATIONS FOR T-CELL RECEPTOR ENGAGEMENT AND T-CELL IMMUNODOMINANCE*[S]

Received for publication, March 21, 2005, and in revised form, April 19, 2005
Published, JBC Papers in Press, April 22, 2005, DOI 10.1074/jbc.M503060200

Fleur E. Tynan‡§¶, Natalie A. Borg‡§, John J. Miles‖, Travis Beddoe‡*, Diah El-Hassen**, Sharon L. Silins‖, Wendy J. M. van Zuylen‖, Anthony W. Purcell**‡‡, Lars Kjer-Nielsen**, James McCluskey**, Scott R. Burrows‖§§¶¶, and Jamie Rossjohn‡§§‖‖**

*From the ‡Protein Crystallography Unit, Department of Biochemistry and Molecular Biology, School of Biomedical Sciences, Monash University, Clayton, Victoria 3800, Australia, the ‖Cellular Immunology Laboratory, Queensland Institute of Medical Research, Brisbane 4029, Australia, and the **Department of Microbiology and Immunology, University of Melbourne, Parkville, Victoria 3010, Australia*

Although HLA class I alleles can bind epitopes up to 14 amino acids in length, little is known about the immunogenicity or the responding T-cell repertoire against such determinants. Here, we describe an HLA-B*3508-restricted cytotoxic T lymphocyte response to a 13-mer viral epitope (LPEPLPQGQLTAY). The rigid, centrally bulged epitope generated a biased T-cell response. Only the N-terminal face of the peptide bulge was critical for recognition by the dominant clonotype SB27. The SB27 public T-cell receptor (TcR) associated slowly onto the complex between the bulged peptide and the major histocompatibility complex, suggesting significant remodeling upon engagement. The broad antigen-binding cleft of HLA-B*3508 represents a critical feature for engagement of the public TcR, as the narrower binding cleft of HLA-B*3501^{LPEPLPQGQLTAY}, which differs from HLA-B*3508 by a single amino acid polymorphism (Arg^{156} → Leu), interacted poorly with the dominant TcR. Biased TcR usage in this cytotoxic T lymphocyte response appears to reflect a dominant role of the prominent peptide·major histocompatibility complex class I surface.

Cytotoxic T lymphocytes (CTLs)[1] recognize short peptide fragments (1, 2), usually 8–10 amino acids in length, complexed to major histocompatibility complex class I (MHC-I) molecules (pMHC-I) (3, 4). Foreign peptides presented to CTLs make specific side chain interactions with anchor sites in the MHC-I binding groove (5). MHC-I can ligate a diverse array of antigenic peptides because of the high degree of polymorphism within the six pockets of the antigen-binding cleft (6). Selection of peptides that bind the MHC-I cleft is usually determined by only two pockets that specify primary anchor sites (7) with one or more secondary anchor sites that fine-tune the binding motifs for individual MHC-I allotypes (8). For example, the common MHC-I molecule HLA-B35 preferentially binds peptide ligands with proline as a dominant anchor residue at position 2 (P2) and generally a tyrosine at the C terminus (PΩ) (9–11). In addition, secondary anchor positions can also influence allele-specific binding (3, 9, 12, 13). MHC-I polymorphism not only diversifies selection of antigens (8), but also broadens the T-cell repertoire that is used to recognize pathogens (14–17). Even single amino acid differences in MHC molecules can exert significant effects on T-cell repertoire selection, patterns of alloreactivity, peptide ligand selection, antigen processing, and susceptibility to viral pathogens (17–19).

In general, the size limitation of peptides that bind to MHC-I is dictated by a hydrogen bonding network, highly conserved between different class I molecules, at the N- and C-terminal ends of the antigen-binding cleft (20–22). Nevertheless, despite these restrictions, some longer peptides can bind to MHC-I (23–29). These longer epitopes can either extend beyond the conventional C-terminal anchor site (29, 30) or bulge centrally from the antigen-binding cleft (25, 28, 31). An extreme example of accommodating a lengthy class I-restricted peptide was observed in rat MHC-I RT1-A^a complexed to a 13-mer epitope, MTF-E (25). The crystal structure of this binary complex reveals a highly solvent-exposed, centrally bulged peptide that displays sufficient mobility to adopt two different conformations within the antigen-binding cleft. Solvent-exposed saccharide residues in glycopeptides presented by MHC molecules have also been observed to protrude substantially from the

* This work was supported in part by the National Health and Medical Research Council, the Australian Research Council, the Juvenile Diabetes Research Foundation, and the Roche Organ Transplantation Research Foundation. The costs of publication of this article were defrayed in part by the payment of page charges. This article must therefore be hereby marked "*advertisement*" in accordance with 18 U.S.C. Section 1734 solely to indicate this fact.

[S] The on-line version of this article (available at http://www.jbc.org) contains a supplemental figure.

The atomic coordinates and structure factors (codes 1ZHK and 1ZHL) have been deposited in the Protein Data Bank, Research Collaboratory for Structural Bioinformatics, Rutgers University, New Brunswick, NJ (http://www.rcsb.org/).

§ Both authors contributed equally to this work.

¶ Supported by an Australian Postgraduate Award scholarship.

‡‡ C. R. Roper Fellow of the University of Melbourne.

§§ Joint senior authors.

¶¶ Supported by a career development award from the National Health and Medical Research Council. To whom correspondence may be addressed. Tel.: 617-3845-3793; Fax: 617-3845-3510; E-mail: scottb@qimr.edu.au.

‖‖ Supported by a Wellcome Trust senior research fellowship in biomedical science in Australia. To whom correspondence may be addressed. Tel.: 613-9905-3736; Fax: 613-9905-4699; E-mail: Jamie.Rossjohn@med.monash.edu.au.

*** Supported by a Peter Doherty fellowship from the National Health and Medical Research Council.

[1] The abbreviations used are: CTLs, cytotoxic T lymphocytes; MHC-I, major histocompatibility complex class I; pMHC, peptide·major histocompatibility complex; TcR, T-cell receptor; EBV, Epstein-Barr virus; PHA, phytohemagglutinin; PBMCs, peripheral blood mononuclear cells; rIL-2, recombinant interleukin-2; CDR3, complementarity-determining region 3; TAP, transporter associated with antigen processing.

peptide-binding groove (32). Recently, unusually long MHC-II-restricted epitopes have been shown to adopt a β-hairpin structure at the C-terminal end of the peptide-binding groove (33); however, this has not been observed for longer class I peptides.

Despite the description of unusually long self-peptides being naturally presented, the role of longer epitopes in antiviral immunity is poorly understood. The prevalence of such epitopes in immunity and the factors governing the processing and presentation of these epitopes are largely unknown. Moreover, how a T-cell receptor (TcR) engages such a pMHC complex and the nature of the T-cell repertoire elicited from such a unique pMHC complex are unknown. However, it has been suggested that prominently bulged peptides may prevent many TcRs from approaching the surface of the MHC molecule, thereby limiting the potential immunogenicity of unusually long class I-binding antigenic peptides (28). Consistent with this view, immunodominant viral epitopes >11 amino acids in length have not been well described in antiviral $CD8^+$ T-cell responses.

To begin to address such issues, we have investigated the immune response to Epstein-Barr virus (EBV), a ubiquitous human pathogen. The CTL response to the very immunogenic lytic antigen BZLF1 includes a cluster of three overlapping sequences of different lengths, a 9-mer (^{56}LPQGQLTAY^{64}), an 11-mer (^{54}EPLPQGQLTAY^{64}), and a 13-mer (^{52}LPEPLPQGQLTAY^{64}), that may form HLA-B*3501-restricted epitopes (27). All peptides bind well to HLA-B*3501; however, the CTL response in individuals expressing this allotype is directed exclusively toward the 11-mer (27). However, the 13-mer epitope (LPEPLPQGQLTAY) is the exclusive target for the CTL response in individuals expressing the HLA-B*3508 allele, which differs from HLA-B*3501 by a single $Leu^{156} \rightarrow Arg$ substitution (27). The above observations are examples of peptide immunodominance (27). In this study, we provide a structural basis for the presentation of long HLA-B35-restricted epitopes and show the restricted nature of the T-cell response (T-cell immunodominance) to these unusual ligands.

EXPERIMENTAL PROCEDURES

Cell Lines—Lymphoblastoid cell lines were established by exogenous transformation of peripheral B-cells with EBV derived from the supernatant of the B95.8 cell line and were maintained in growth medium (10% fetal calf serum and RPMI 1640 medium). The mutant lymphoblastoid cell line × T lymphoblastoid hybrid cell line 174xCEM.T2 (referred to as T2 cells) (34), expressing HLA-B*3508 (T2.B*3508) (27, 35), was also used in this study. Phytohemagglutinin (PHA) blasts were generated by stimulating peripheral blood mononuclear cells (PBMCs) with PHA (Sigma), and after 3 days, growth medium containing supernatant from the interleukin-2-producing cell line MLA-144 (European Collection of Cell Cultures) and recombinant interleukin-2 (rIL-2) were added. PHA blasts were propagated with biweekly replacement of rIL-2 and MLA-144 supernatant (PHA-free) for up to 8 weeks. The blood donors used in this study were healthy laboratory staff selected for particular HLA alleles, and prior exposure to EBV was assessed by standard virus-specific antibody tests. All cell lines were regularly screened for mycoplasma contamination.

CTL Cultures—CTL clones were generated by agar cloning as follows. PBMCs (2×10^6) were stimulated in 2 ml of growth medium with autologous PBMCs that had been precoated with the LPEPLPQGQLTAY peptide at 1 μM for 1 h (responder/stimulator ratio of 2:1). After 3 days, cells were dispersed and seeded on 0.35% (w/v) agarose (Seaplaque, BioWhittaker Molecular Applications, Rockland, ME) containing RPMI 1640 medium, 20% (v/v) fetal calf serum, and 25% (v/v) supernatant from MLA-144 cultures and rIL-2 (50 units/ml). Colonies were harvested after an additional 3–5 days and amplified in culture with biweekly restimulation with rIL-2, MLA-144 supernatant, and γ-irradiated (8000 rads) autologous lymphoblastoid cell lines that had been prelabeled with the LPEPLPQGQLTAY peptide at 0.1 μM for 1 h and washed three times.

Cytotoxicity Assay/Fine Specificity Analysis—CTL cultures were tested in duplicate or triplicate for cytotoxicity in a standard 5-h chromium release assay. Briefly, CTLs were assayed against ^{51}Cr-labeled PHA blast targets that were pretreated with synthetic peptide or left untreated. Percent specific lysis was calculated, and the peptide concentration required for half-maximum lysis was determined from dose-response curves. To reduce spontaneous lysis of PHA blast target cells, the medium used in the chromium release assays was supplemented with rIL-2. Peptides were synthesized by Mimotopes Ltd. (Clayton, Victoria, Australia). Toxicity testing of all peptides was performed prior to use by adding peptide to ^{51}Cr-labeled PHA blasts in the absence of CTL effectors. A β-scintillation counter (Topcount Microplate, Packard Instrument Co.) was used to measure ^{51}Cr levels in assay supernatant samples. The mean spontaneous lysis for target cells in the culture medium was always <20%, and the variation about the mean specific lysis was <10%.

Flow Cytometric Analysis—PBMCs or bulk T-cell cultures were incubated for 30 min at 4 °C with a phycoerythrin-labeled HLA-B*3508^{LPEPLPQGQLTAY} tetramer (Proimmune Ltd., Oxford, UK). Cells were then washed and labeled for 30 min at 4 °C with TRI-COLOR®-labeled anti-human CD8 antibody (Caltag Laboratories, Burlingame, CA), allophycocyanin-labeled anti-human CD3 antibody (Pharmingen), and one of the following fluorescein isothiocyanate-labeled TcRβ chain-specific antibodies (Serotec, Oxford): Vβ1 (TRBV9), Vβ2 (TRBV20-1), Vβ3 (TRBV28), Vβ5.1 (TRBV5-1), Vβ5.2 (TRBV5-6), Vβ5.3 (TRBV5-5), Vβ6.7 (TRBV7-1), Vβ7 (TRBV4), Vβ8 (TRBV12), Vβ11 (TRBV25-1), Vβ12 (TRBV10), Vβ13.1 (TRBV6-5), Vβ13.6 (TRBV6-6), Vβ14 (TRBV27), Vβ16 (TRBV14), Vβ17 (TRBV19), Vβ18 (TRBV18), Vβ20 (TRBV30), Vβ21.3 (TRBV11-1), Vβ22 (TRBV2), or Vβ23 (TRBV13). Cells were washed and analyzed by flow cytometry on a FACSCalibur using CellQuest software (BD Biosciences). Cell sorting was performed on a MoFlo high proficiency cell sorter (Cytomation, Inc., Fort Collins, CO).

T-cell Repertoire Analysis—T-cell clones were verified for purity and peptide specificity by flow cytometry with an HLA-B*3508^{LPEPLPQGQLTAY} tetramer before TcR analysis was performed. Total RNA was extracted from T-cell clones and tetramer sorted bulk CTL cultures using TRIzol reagent. Reverse transcription was performed with Superscript III (Invitrogen) and antisense TcRα and TcRβ chain primers. PCR was performed in a 25-μl volume consisting of 200 μM dNTPs, 20 mM $MgCl_2$, and 1.25 units of AmpliTaq Gold (Applied Biosystems, Foster City, CA) using a TcRβ constant primer and 1 of 24 TcRβ V family-specific primers or a TcRα C constant primer and 1 of 34 TcRα V family-specific primers (36). PCR products were purified and ligated into the pGEM-T vector system (Promega Corp., Madison, WI) and sequenced using the ABI PRISM BigDye terminator reaction kit (Applied Biosystems). Nomenclature for TcR usage is based on the International ImMunoGeneTics Information System (37).

Expression, Purification, and Crystallization of HLA-B35 Alleles in Complex with Long Epitopes—Soluble HLA-B*3501 and HLA-B*3508 molecules (residues 1–276) and full-length β_2-microglobulin (residues 1–99) were expressed, refolded with the LPEPLPQGQLTAY peptide, purified, and concentrated to 10 mg/ml as described previously (38). The HLA-B35 crystals were obtained by the hanging drop vapor diffusion technique. Large (0.7 × 0.5 × 0.3 mm) block-shaped crystals grew within 5 days in 0.2 M ammonium acetate and 17% (w/v) polyethylene glycol 3350 (100 mM cacodylate (pH 7.6)) at 4 °C.

X-ray Data Collection and Structure Determination—Crystals were directly transferred to cryoprotectant-containing 20% glycerol and flash-frozen prior to data collection. Data were collected on an in-house radiation source and at the Advanced Photon Source (Argonne National Laboratory, Argonne, IL). Data were processed and scaled using the HKL suite (see Table I) (39).

The HLA-B35 complex structures were refined from an HLA-B*3501 structure that was previously determined in our laboratory.[2] The model was manually built using program O (40) and improved through multiple rounds of refinement using the CNS suite (41). The progress of refinement was monitored by R_{fac} and R_{free} values. Rigid body refinement and simulated annealing were used in the first instance, but in later rounds, energy minimization and *B*-individual refinement were used to improve the quality of the model. See Table I for the final refinement and model statistics.

TcR Cloning, Expression, and Refolding—The genes encoding TRAV19 and TRBV6-1 were cloned from the HLA-B*3508-restricted, 13-mer-specific T-cell clone SB27. DNA encoding the extracellular domains of TRAV19 and TRBV6-1 and terminating immediately before the interchain extracellular cysteines was cloned into the pET30 ex-

[2] N. A. Borg, J. Rossjohn, S. R. Burrows, and J. McCluskey, unpublished data.

TABLE I
Data collection and refinement statistics
Values in parentheses are for the highest resolution shell. r.m.s., root mean square.

	HLA-B*3501·13-mer	HLA-B*3508·13-mer
Data collection		
Peptide	LPEPLPQGQLTAY	LPEPLPQGQLTAY
Temperature	100 K	100 K
Space group	$P2_12_12_1$	$P2_12_12_1$
Cell dimensions (*a, b, c*) (Å)	51.25, 81.75, 110.42	50.81, 81.34, 111.00
Resolution (Å)	30 to 1.6	30 to 1.5
Total no. observations	217,659	204,388
No. unique observations	60,254	68,753
Data completeness (%)	96.7 (84)	92.1 (82.8)
No. data $> 2\sigma_I$	78.7 (39.1)	82.2 (56.6)
I/σ_I	19.6 (2.1)	20.6 (4.3)
R_{merge} (%)[a]	6.5 (48.5)	6.2 (30.6)
Refinement statistics		
Non-hydrogen atoms		
Protein	3184	3187
Water	448	610
Resolution (Å)	1.6	1.5
R_{factor} (%)[b]	21.9	20.3
R_{free} (%)[c]	23.1	22.7
r.m.s. deviations from ideality		
Bond lengths (Å)	0.007	0.004
Bond angles	1.62°	1.24°
Dihedrals	25.14°	24.64°
Impropers	0.88°	0.74°
Ramachandran plot		
Most favored	90.5	92.9
And allowed region (%)	9.2	7.1
Disallowed[d]	0.3	0
B-factors (Å^2)		
Average main chain	18.42	13.52
Average side chain	21.16	16.22
Average water molecule	31.67	27.86
Average peptide	23.10	15.79
r.m.s. deviation bonded Bs	1.67	1.59

[a] $R_{merge} = \Sigma|I_{hkl} - \langle I_{hkl}\rangle|/\Sigma I_{hkl}$.
[b] $R_{factor} = \Sigma_{hkl}\| F_o| - |F_c\|/\Sigma_{hkl}|F_o|$ for all data except as indicated in Footnote *c*.
[c] 3.9 and 3.7% were used for the R_{free} calculation for the HLA-B*3501·13-mer and HLA-B*3508·13-mer, respectively.
[d] This residue is in a region of poor electron density.

pression vector (Novagen). DNA encoding the unpaired cysteine at position 77 of TRBV6-1 was mutated to encode an alanine. Additionally, DNA was mutated to encode a cysteine in the constant domain of both TRAV19 ($Thr^{48} \rightarrow Cys$) and TRBV6-1 ($Ser^{57} \rightarrow Cys$) (75). TRAV19 and TRBV6-1 were expressed, refolded, and purified as described previously (76), except that the protein was refolded in the presence of 5 M urea.

Biacore Measurements and Analysis—All surface plasmon resonance experiments were carried out at 25 °C on a Biacore 3000 instrument using 10 mM HEPES-HCl (pH 7.4), 150 mM NaCl, and 0.005% (v/v) surfactant P20 (supplied by the manufacturer) supplemented with 1% (w/v) bovine serum albumin to inhibit nonspecific binding. Antibody 12H8 (42) was coupled to research-grade CM5 chips using standard amine coupling at a level of 9000–11,000 response units. For each experiment, 400–600 response units of SB27 was captured on the antibody. MHC (1–56.2 μM) was injected over all flow cells at 20 μl/min. The final response was calculated by subtraction of the response to the antibody alone from the response to the antibody·TcR complex. The antibody surface was regenerated between each analyte injection using ActiSep (Sterogene Bioseparations Inc.). BIAevaluation Version 3.1 (Biacore) was used for data analysis; the 1:1 Langmuir binding model was used to calculate the kinetic constants. To allow for the capture system, the model was modified to include an additional parameter for the drifting base line and local fitting of the binding maxima. The calculated K_d ($K_{d(calc)}$; k_{off}/k_{on}) concurred with the equilibrium dissociation constant ($K_{d(eq)}$) for all reported values. This experiment was performed twice.

To further support this result, the reverse experiment was performed, in which HLA-B*3501^{LPEPLPQGQLTAY} and HLA-B*3508^{LPEPLPQGQLTAY} were coupled to different flow cells on research-grade CM5 chips using the MHC-specific antibody W6/32 (43), and the SB27 TcR (1–56.2 μM) was injected at 20 μl/min over all flow cells. Blanks were subtracted, and data were examined as described above.

Similar results for all experiments ($n = 3$) were obtained. The means ± S.E. were determined.

RESULTS

Crystal Structures of HLA-B35 Complexed to Unusually Long Viral Epitopes—To address the structural basis of binding of long epitopes to HLA-B35, we determined the crystal structure of the immunogenic HLA-B*3508^{LPEPLPQGQLTAY} complex to 1.5-Å resolution (R_{fac} = 20.3%, R_{free} = 22.7%) and the non-immunogenic HLA-B*3501^{LPEPLPQGQLTAY} complex to 1.6-Å resolution (R_{fac} = 21.9%, R_{free} = 23.1%) (Table I). The two complexes crystallize in the same space group under identical conditions with isomorphous unit cells; and notably, the bound epitopes do not participate in crystal contacts. Accordingly, conformational differences that are observed between the two crystal structures can be attributed to the polymorphic amino acid at position 156. The electron density for the bound peptides was very clear in the HLA-B*3501^{LPEPLPQGQLTAY} and HLA-B*3508^{LPEPLPQGQLTAY} structures (Fig. 1, *A* and *B*). The features of the HLA-B*3508^{LPEPLPQGQLTAY} complex are discussed first, followed by the salient aspects of the other binary complex.

The LPEPLPQGQLTAY epitope is bound in the bulged mode, with the N and C termini anchored in the A- and F-pockets, respectively; 11 of the 12 direct hydrogen bonds between the peptide and HLA-B*3508 are located within these pockets (Table II). The P1–C-α/PΩ–C-α distance is 21.9 Å in the HLA-B*3508^{LPEPLPQGQLTAY} complex (Fig. 1*C*), which compares closely with the P1–C-α/PΩ–C-α distance observed in the previously determined octameric and nonameric HLA-B*3501 complexes (44, 45). The P1-Leu binds in a standard class I binding mode within the A-pocket, differing from that previously observed in the octameric HLA-B*3501 complex. The

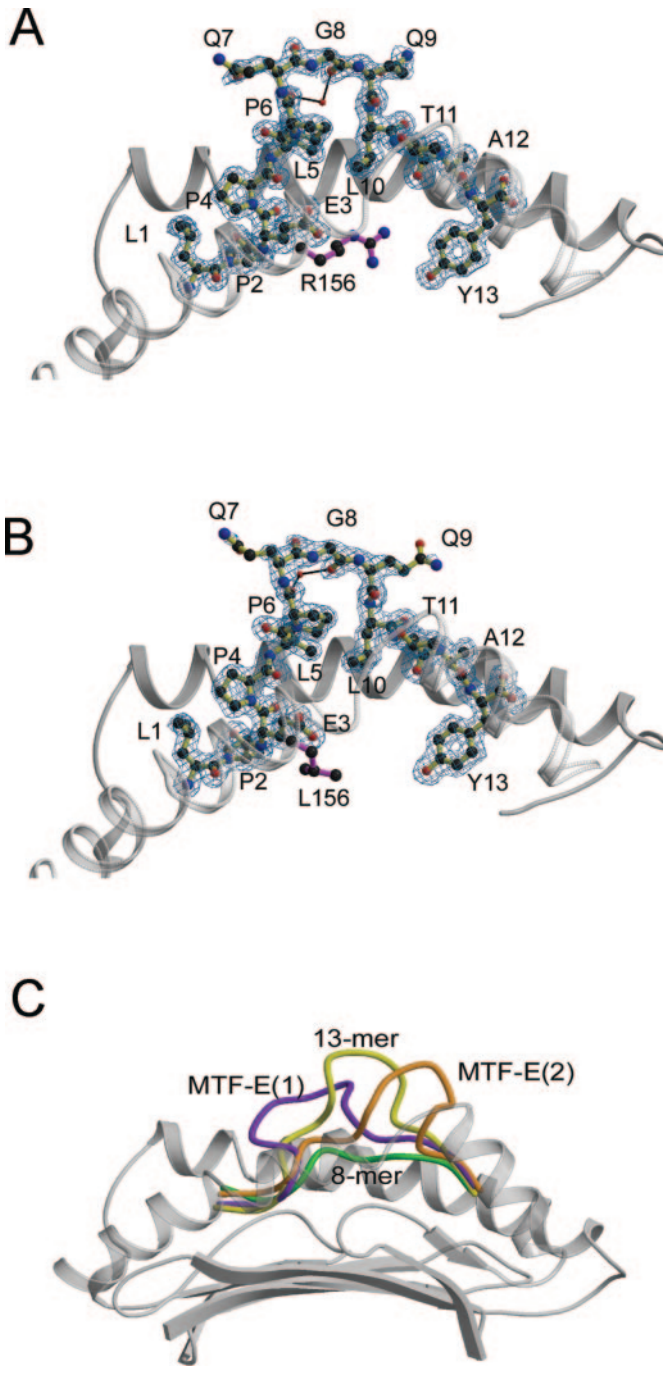

FIG. 1. **Structures of bulged epitopes complexed to MHC-I.** $2F_o - F_c$ electron density is shown in mesh format, with residues shown in *ball-and-stick* format. The polymorphic residue is shown in *purple*. A water molecule bridging the bulged loop is shown. *A* and *B*, structures of HLA-B*3508 and HLA-B*3501, respectively, complexed to LPEPLPQGQLTAY. *C*, superposition of the bulged epitopes bound to MHC-I compared with an 8-mer epitope. The 13-mer (this work) is shown in *yellow*, and the 8-mer peptide (45) shown in *green*. The MTF-E epitope is observed in two different conformations (25), shown in *purple* and *orange*.

nonstandard positioning of the PΩ residue, initially observed in the octameric HLA-B*3501 complex (45), is also present in the HLA-B*3508^{LPEPLPQGQLTAY} complex; this indicates that the mode of binding within the PΩ pocket is a characteristic of HLA-B35 and is independent of peptide length. The P2-Pro binding pocket, an anchor motif for HLA-B35, is conserved between this structure and that described previously (45). Notably, there is a large network of water-mediated hydrogen bonds between HLA-B*3508 and the LPEPLPQGQLTAY epitope, which may partly assist in stabilizing this epitope within the binding groove (Table II); many of these water molecules reside in the space normally occupied by the central region of the 8/9-mer peptides bound to HLA-B35.

The 13-mer epitope protrudes above the antigen-binding cleft to such an extent that the extreme tip of the bulged region of the peptide is ~10 Å higher in the peptide-binding groove in comparison with the octameric HLA-B35 complex (45) (Fig. 1*C*). 34.8% of the 13-mer is solvent-exposed when bound to HLA-B*3508, compared with only 18.6 and 25.0% for the previously described octameric and nonameric HLA-B35 complexes, respectively. Despite residues P5–P9 of the epitope making minimum direct contacts with HLA-B*3508, these residues exhibit average temperature factors of only 14.5, 17.9, 31.0, 25.0, and 27.4 Å^2, respectively, which compares with the average temperature factors of 15.8 and 14.9 Å^2 for the entire 13-mer epitope and the entire HLA-B*3508^{LPEPLPQGQLTAY} complex, respectively. The presence of three proline residues (P2-Pro, P4-Pro, and P6-Pro) within the N-terminal region of the peptide not only serves to raise the peptide out of the cleft, but also provides rigidity to the bulged region of the epitope (Fig. 1, *A* and *B*). In addition, the bulged epitope is stabilized by residues P6–P9 forming a type IV β-turn that enables the P6-Pro side chain to pack against P10-Leu. Moreover, the bulged region of the peptide is stabilized by intrapeptide water-mediated hydrogen bonds as well as water-mediated hydrogen bonds to HLA-B*3508. For example, a water molecule bridges the carbonyl groups between P6 and P8 of the peptide (Fig. 1, *A* and *B*).

Selection of T-cells Specific for the LPEPLPQGQLTAY Viral Epitope Is Controlled by a Single Residue Polymorphism on the α2 Helix of the Class I Heavy Chain—HLA-B*3508 differs from HLA-B*3501 by a single amino acid (Leu^{156} → Arg), yet CTLs recognizing the HLA-B*3501^{LPEPLPQGQLTAY} complex are not detected in the immune response to EBV in HLA-B*3501$^+$ individuals. To evaluate the structural basis of the influence of polymorphism on the immunogenicity of the BZLF1-derived 13-mer, we compared the crystal structures of the HLA-B*3508 and HLA-B*3501 binary complexes bound to the LPEPLPQGQLTAY epitope (Fig. 2).

Analogous to the HLA-B*3508^{LPEPLPQGQLTAY} complex, the HLA-B*3501^{LPEPLPQGQLTAY} complex exhibits ordered electron density for the entire epitope, despite HLA-B*3501 making fewer contacts with the base of the epitope as a direct result of the Arg^{156} → Leu polymorphism (Fig. 1*B* and Table II). This observation correlates with HLA-B*3508^{LPEPLPQGQLTAY} being 4 °C more thermostable than HLA-B*3501^{LPEPLPQGQLTAY} (data not shown). The conformation of the bound peptide in the two structures is very similar (root mean square deviation of 0.24 Å over 13 C-α atoms), but in relation to the antigen-binding cleft, the tip (P7–P9) of the bulged loop in the HLA-B*3508 complex is shifted away from the structurally conserved α1 helix by 0.6–0.9 Å (Fig. 2*A*). The HLA-B*3501^{LPEPLPQGQLTAY} and HLA-B*3508^{LPEPLPQGQLTAY} complexes superpose well (root mean square deviation of 0.37 Å over 180 C-α atoms of the heavy chain); the largest structural differences (>0.5 Å at C-α) are observed at positions 105–109, 145–152, 155, 156, and 158 (Fig. 2*A*). Residues 105–109 represent a flexible loop, remote from the peptide-binding site, the conformation of which is influenced by crystal contacts. However, the structural differences in region 145–158 of the α2 helix are a result of the polymorphism at position 156 between HLA-B*3501 and HLA-B*3508.

In HLA-B*3508, Arg^{156} forms an integral part of an unusual charged cluster of residues, with its guanidinium group stacking antiparallel to the guanidinium group of Arg^{97} (Fig. 2*B*). This interaction is flanked by two salt bridging residues, Asp^{114} located within the F-pocket and the P3-Glu from the peptide.

TABLE II
*HLA-B*3508 contacts with the LPEPLPQGQLTAY epitope*

Peptide residue	MHC	Type of bond	08/01 differences
Leu[1] O	Tyr[159] OH	H-bond	
Leu[1] N	Tyr[171] OH, Tyr[7] OH	H-bond	
Leu[1]	Arg[62], Asn[63], Trp[167]	VDW[a]	
Pro[2]	Tyr[7], Asn[63], Ile[66], Tyr[99], Tyr[159]	VDW	
Glu[3] N	Tyr[99] OH	H-bond	
Glu[3] N	Tyr[9] OH	Water-mediated	
Glu[3] O	Tyr[9] OH, Asn[70] N-δ2	Water-mediated	
Glu[3] O-ε1	Arg[97] NH1,NH2	Salt bridge	
Glu[3] O-ε1	Arg[156] N-ε	Salt bridge, water-mediated	08
Glu[3] O-ε1	Asp[114] O-δ2	Water-mediated	01
Glu[3] O-ε2	Gln[155] O-ε1	Water-mediated	08
Glu[3] O-ε2	Ala[152] O	Water-mediated	01
Glu[3]	Tyr[159], Ile[66]	VDW	
Pro[4] O	Asn[70] N-δ2	Water-mediated	
Pro[4]	Ile[66], Tyr[159], Leu[163]	VDW	
Leu[5] N	Arg[62] N-ε, O, Gln[155] O-ε1	Water-mediated	
Leu[5]	Thr[69]	VDW	
Pro[6]	Gln[155]	VDW	
Gln[9] O	Gln[155] N-ε2	Water-mediated	
Gln[9] O-ε1	Thr[73] O-γ1	Water-mediated	08
Gln[9] O-ε1	Glu[76] O-ε1, O-ε2	Water-mediated	01
Leu[10] O	Thr[73] O-γ1	Water-mediated	
Leu[10]	Asn[70], Thr[73]	VDW	
Thr[11] O-γ1	Gln[155] O-ε1	Water-mediated 2 bridging in 01	
Thr[11] N	Gln[155] O-ε1	Water-mediated	
Thr[11] O	Arg[156] NH2	Water-mediated	08
Thr[11]	Ala[150], Val[152], Lys[146], Trp[147]	VDW	
Ala[12] O	Trp[147] N-ε1	H-bond	
Ala[12] N	Glu[76] O-ε2, Lys[146] N-ζ	Water-mediated	
Ala[12]	Thr[73], Ser[77], Glu[76], Lys[146], Trp[147]	VDW	
Tyr[13] N	Ser[77] O-γ	H-bond	
Tyr[13] OH	Tyr[74] OH, Ser[116] O-γ	H-bond	
Tyr[13] OH	Arg[156] NH1, Asp[114] O-δ1, Ser[116] O-γ	Water-mediated	08
Tyr[13] O	Asn[80] O-δ1, Lys[146] N-ζ	H-bond	
Tyr[13] OXT	Thr[143] O-γ1, Tyr[84] OH	H-bond	
Tyr[13]	Tyr[74], Ser[77], Asn[80], Leu[81], Ile[95], Ser[116], Tyr[123], Thr[143], Trp[147]	VDW	

[a] VDW, van der Waals.

The extended conformation of the aliphatic moiety of Arg[156] is further stabilized by van der Waals interactions with Leu[126], Trp[133], and Val[152]. Arg[156] also participates in a number of water-mediated interactions, which is due principally to the water-filled cavity created by the central region of the peptide arching upwards out of the cleft (Fig. 2*B*). These interactions include a water-mediated hydrogen bond from Arg[156] N-ϵ to P3-Glu O-ϵ2 and Gln[155] O-ϵ1, a water-mediated hydrogen bond from Arg[156] NH1,NH2 to Asp[114] and Ser[116] O-γ, and another water molecule that bridges to P13-Tyr OH (Fig. 2*B*). In HLA-B*3501, the positively charged Arg at position 156 is replaced with the hydrophobic Leu residue, resulting in van der Waals interactions now dominating this position. Leu[156] forms van der Waals contacts with Leu[126], Val[152], Leu[160], and the aliphatic moiety of Asp[114] (Fig. 2*C*). In addition, Leu[156] forms unfavorable van der Waals interactions with P3-Glu and Arg[97], the charges of which are presumably dissipated by the Asp[114], Arg[97], and P3-Glu interaction network.

To accommodate this polymorphic residue at position 156, there are a number of localized conformational changes. First, Val[152] in HLA-B*3508 moves away from the positively charged Arg[156]. Second, in HLA-B*3501, Leu[156] points toward the floor of the antigen-binding cleft, whereas in HLA-B*3508, Arg[156] runs parallel with the floor of the antigen-binding cleft (Fig. 2, *A–C*). To avoid unfavorable interactions with the hydrophobic Leu[156], the carboxylate moiety of Asp[114] rotates ~80° away and forms a more favorable interaction with Arg[97] (Fig. 2*C*). Third, to compensate partly for the loss of the salt bridge between P3-Glu and position 156 in HLA-B*3501, the P3-Glu forms a water-mediated hydrogen bond with main chain of Val[152] (Fig. 2*C*). In addition, the extensive network of water-mediated hydrogen bonds emanating from position 156 is lost in HLA-B*3501. These conformational changes culminate in a 1-Å rigid body shift within the prominent ridge (positions 145–152) of the α2 helix, in which Val[152] acts as the seed point for this rigid body conformational change (Fig. 2*A*).

TcR Immunodominance in the Recognition of the Bulged 13-mer Determinant—Most pMHC complexes protrude minimally from the plane of the antigen-binding cleft and provide a limited number of solvent-exposed peptide side chains for TcR interaction. In contrast, the 13-mer determinant exposes a highly bulged region that poses a structural challenge for conventional T-cell recognition. Therefore, we examined the repertoire of T-cell clonotypes in the HLA-B*3508-restricted, 13-mer-specific CTL population. To determine the TcR usage, a panel of Vβ-specific monoclonal antibodies was screened against HLA-B*3508^{LPEPLPQGQLTAY} tetramer-expressing CD8$^+$ cells (Fig. 3). In all three donors tested, the T-cell response to the highly immunogenic HLA-B*3508^{LPEPLPQGQLTAY} complex (0.41–2% CD8$^+$ cells) was markedly restricted in Vβ usage. The response in donor J. W. was dominated by TRBV20-1 and TRBV27, whereas donors C. A. and S. B. had in common a large expansion of TRBV5-6. TcR sequence analysis of HLA-B*3508^{LPEPLPQGQLTAY}-specific T-cell clones confirmed

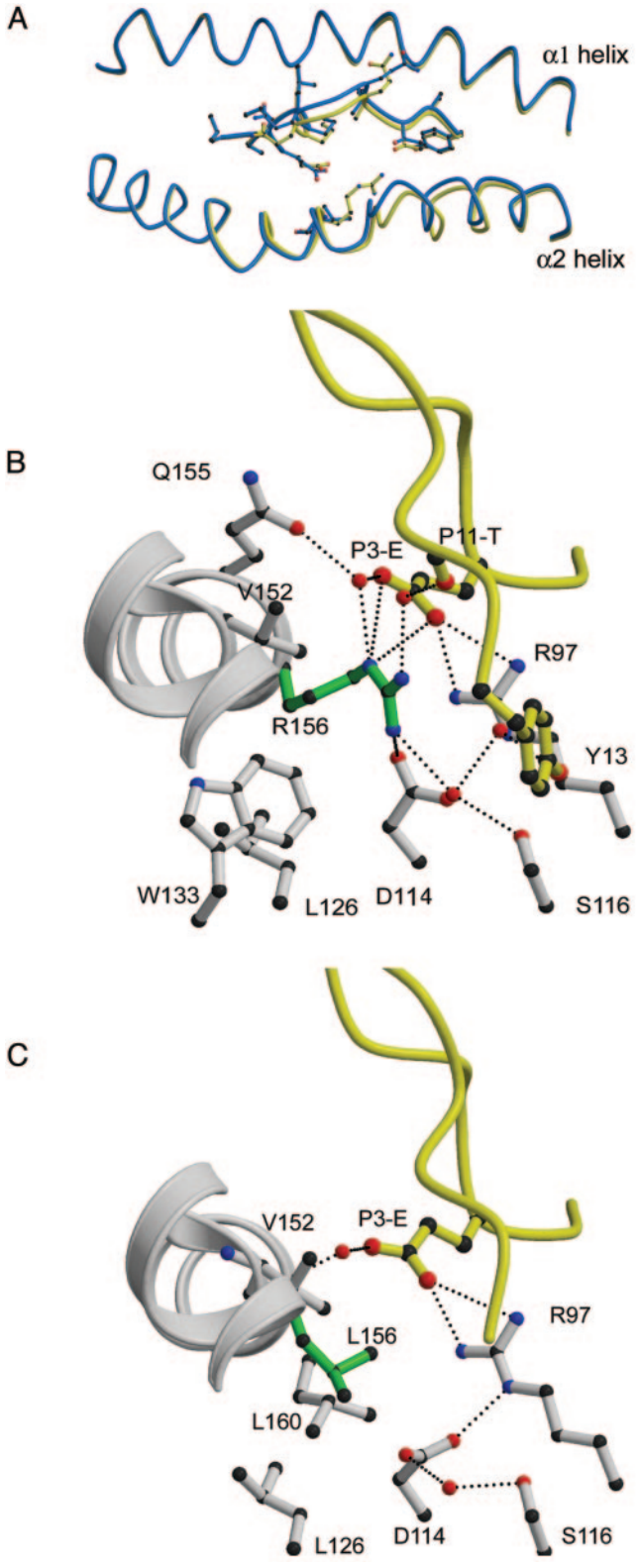

FIG. 2. *A*, superposition of the two antigen-binding clefts, HLA-B*3508 (*yellow*) and HLA-B*3501 (*blue*), highlighting the shift in the α2 helix spanning residues 145–158. *B* and *C*, impact of the polymorphism at position on the local structure of HLA-B*3508^{LPEPLPQGQLTAY} and HLA-B*3501^{LPEPLPQGQLTAY}, respectively. Residues are in *ball-and-stick* format. Polar interactions are depicted as *dotted lines*. The polymorphic residue is shown in *green*, and the peptide is shown in *yellow*.

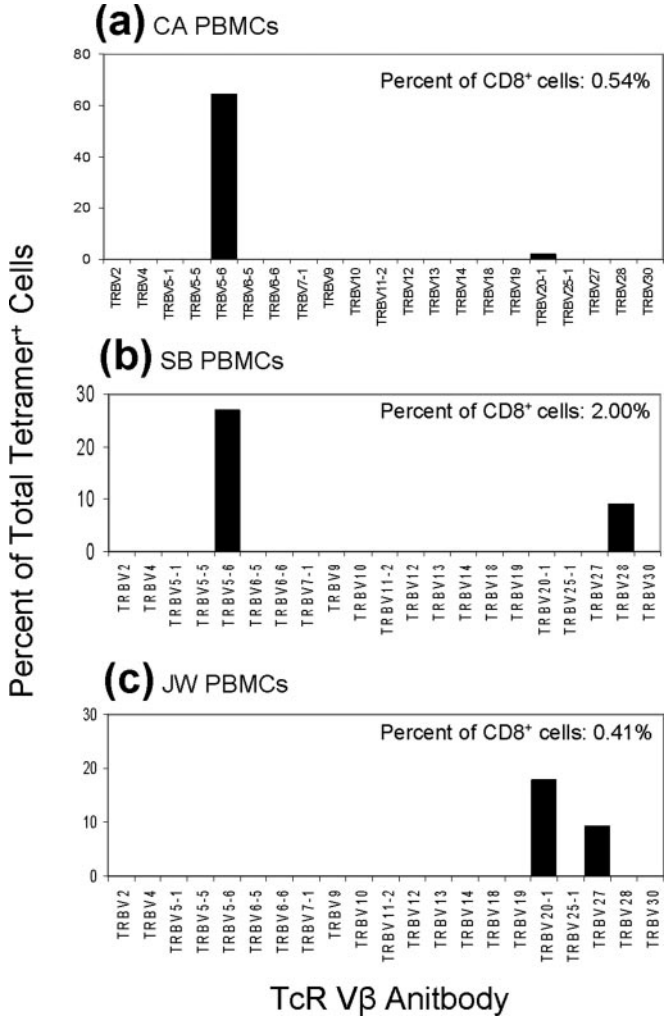

FIG. 3. **The repertoire of TcRβ chains utilized against the EBV LPEPLPQGQLTAY epitope is restricted.** PBMCs from the EBV-seropositive HLA-B*3508^{+} donors C. A. (*a*), S. B. (*b*), and J. W. (*c*) were co-stained with the HLA-B*3508^{LPEPLPQGQLTAY} (*LPEP-B*3508*) tetramer and 1 of 21 TRBV-specific antibodies. Only gated percentages of 0.02% and over were considered significant, and the designation of TRBV follows the International ImMunoGeneTics Information System TcR nomenclature.

the TRBV5-6 usage in donor S. B. and revealed an additional TRBV7-2 contribution in donor S. B. and TRBV6-1 contribution in donors S. B. and C. A. (Tables III and IV). Strikingly, regardless of the type of Vβ expressed, most HLA-B*3508^{LPEPLPQGQLTAY}-specific clones shared an identical or public TRAV19/TRAJ34 chain. Strong selection for this conserved Vα rearrangement in the HLA-B*3508^{LPEPLPQGQLTAY} response was further evident when HLA-B*3508^{LPEPLPQGQLTAY} tetramer-expressing CD8^{+} cells from all three donors were screened for TRAV19 expression (Tables III and IV). In each donor, the public TRAV19/TRAJ34 chain was present at high frequency. Moreover, within donors S. B. and J. W., there existed several independently rearranged clonotypes that varied in codon usage within complementarity-determining region 3 (CDR3), yet expressed identical or nearly identical public TRAV19/TRAJ34 chains. Overall, TcR recognition of the substantially bulged HLA-B*3508^{LPEPLPQGQLTAY} complex appears to be stringently controlled by a subset of CD8^{+} T-cells that share a public α-chain.

*A Critical Role for P4–P7 in the Recognition of the HLA-B*3508^{LPEPLPQGQLTAY} Complex by a Dominant CTL Clonotype*—The crystal structure of the HLA-B*3508^{LPEPLPQGQLTAY} complex reveals a number of prominent sites (P4–P9 and P11) that could potentially interact with the dominant TcRs. To delineate which residues of the epitope participate in TcR interactions, a fine specificity analysis was carried out on a CTL

TABLE III
CDR3 of 13-mer-specific T-cell clones
The designations of TRBV, TRBJ, TRAV, and TRAJ follow the nomenclature of the International ImMunoGeneTics Information System (37).

CTL clone	TcRβ chain				TcRα chain				Frequency[a]
	TRBV	V(D)J	TRBJ	CDR3 length	TRAV	VJ	TRAJ	CDR3 length	
SB9	7–2	CASSIGTGGSQPQHF	1–5	10	19	CALSGFYNTDKLIF	34	9	2/10
SB32	5–6	CASSKLGTSEETQYF	2–5	10	19	CALSGFYNTDKLIF	34	9	1/10
SB27	6–1	CASPGLAGEYEQYF	2–7	9	19	CALSGFYNTDKLIF	34	9	6/10
CA5	6–1	CASPGETEAFF	1–1	6	19	CALSGFYNTDKLIF	34	9	1/1
					10	CVVSCSGNTGKLIF	37	9	1/1
SB47	5–6	CASSRTGSTYEQYF	2–7	9	16	CALRDPTGANSKLTF	56	10	1/10

[a] Frequency of CTL clones expressing a specific TcR.

TABLE IV
CDR3 homology from 13-mer tetramer sorted T-cells
Green areas represent the TcR family germ line, and red areas represent the region germ line.

Donor	TRAV19[a] Sequence														TRAJ[a]	f[b]
	C	A	L	S	G	F	Y	N	T	D	K	L	I	F	34	
CA	tgt	gct	ctg	agt	ggg	ttt	tat	aac	acc	gac	aag	ctc	atc	ttt		17/22
SB	tgt	gct	ctg	agt	ggg	ttt	tat	aac	acc	gac	aag	ctc	atc	ttt		13/15
JW	tgt	gct	ctg	agt	ggg	ttt	tat	aac	acc	gac	aag	ctc	atc	ttt		29/33
SB	tgt	gct	ctg	agt	gga	ttt	tat	aac	acc	gac	aag	ctc	atc	ttt		2/15
JW	tgt	gct	ctg	agt	ggc	ttt	tat	aac	acc	gac	aag	ctc	atc	ttt		3/33
	C	A	L	S	G	F	H	N	T	D	K	L	I	F	34	
JW	tgt	gct	ctg	agt	ggg	ttt	cat	aac	acc	gac	aag	ctc	atc	ttt		1/33
	C	A	L	S	E	A	Y	S	N	D	Y	K	L	S	F	20	
CA	tgt	gct	ctg	agt	gag	gcg	tac	tct	aac	gac	tac	aag	ctc	agc	ttt	5/22

[a] The designations of TRAV and TRAJ follow the nomenclature of the International ImMunoGeneTics Information System (37).
[b] Values signify the frequency of the TcR recovered from HLA-B*3508 ^{LPEPLPQGQLTAY} tetramer sorted CD8$^+$ T-cells.

clone (SB27) that expresses a dominant TcR with the public TRAV19/TRAJ34 α-chain sequence (Fig. 4). CTL reactivity was determined by systematically substituting each residue in the LPEPLPQGQLTAY epitope with either glycine or tyrosine and then assaying their recognition by SB27 CTLs. The peptides with glycine replacements were also tested for binding to HLA-B*3508 using the T2.B*3508 cell line to assist in interpreting the CTL recognition data (Fig. 4). Replacement of Leu^5, Pro^6, and Gln^7 with glycine resulted in greatly reduced CTL recognition (Fig. 4), indicating that these residues are critical determinants for recognition by the SB27 clonotype; this is consistent with the tyrosine replacement data (see supplemental figure), which also indicated that Pro^4, Leu^5, and Gln^7 are important residues for SB27 CTL binding. Thus, the fine specificity analyses revealed that the TcR of the dominant clonotype SB27 recognizes the N-terminal slope of the bulged peptide, whereas the extreme tip and C-terminal half of the bulged peptide are not critical determinants for TcR recognition.

*The Non-immunogenic HLA-B*3501^{LPEPLPQGQLTAY} Complex Has a Low Affinity for the Dominant SB27 TcR*—Given the differential immunogenicity of the HLA-B*3501^{LPEPLPQGQLTAY} and HLA-B*3508^{LPEPLPQGQLTAY} ligands in EBV-infected individuals, we reasoned that large bulged peptides might represent energetically challenging targets recognizable by only a limited number of TcRs, as suggested in the repertoire analysis of HLA-B*3508$^+$ donors. Therefore we compared the affinity and kinetic constants for the interaction of the SB27 TcR with the HLA-B*3508^{LPEPLPQGQLTAY} and HLA-B*3501^{LPEPLPQGQLTAY} complexes (Fig. 5). To achieve this, the soluble ectodomains of the SB27 TcR were expressed and refolded into a native conformation (data not shown). Surface plasmon resonance analysis revealed that the affinity ($K_{d(eq)}$) of the SB27 TcR/HLA-B*3508^{LPEPLPQGQLTAY} interaction was 9.85 ± 0.98 μM, with $K_{d(calc)}$ = 13.57 ± 0.53 μM, an on-rate (k_{on}) of 9300 ± 1374 M^{-1} s^{-1}, and an off-rate (k_{off}) of 0.125 ± 0.014 s^{-1}. Surface plasmon resonance analysis of the SB27 TcR/HLA-B*3501^{LPEPLPQGQLTAY} interaction yielded $K_{d(eq)}$ = 35.23 ± 2.8 μM, $K_{d(calc)}$ = 43.0 ± 8 μM, k_{on} = 7620 ± 1865 M^{-1} s^{-1}, and k_{off} = 0.297 ± 0.019 s^{-1}. Thus, the non-immunogenic HLA-B*3501^{LPEPLPQGQLTAY} complex interacted with the highly selected dominant TcR clonotype at a significantly lower affinity compared with the immunogenic HLA-B*3508^{LPEPLPQGQLTAY} ligand. Notably, the SB27 TcR dissociated more readily from the HLA-B*3501^{LPEPLPQGQLTAY} complex ($t_{½}$ = 2.33 s) than from the HLA-B*3508^{LPEPLPQGQLTAY} complex ($t_{½}$ = 5.54 s) (Fig. 5).

DISCUSSION

We have characterized an immunodominant or so-called "public" CTL response to a non-canonical 13-mer epitope of the EBV BZLF1 antigen. The entire LPEPLPQGQLTAY epitope bound to HLA-B*3501 and HLA-B*3508 is rigid. This is in marked contrast to the flexibility observed in previously determined highly bulged epitopes (25). This rigidity can be attributed to the three proline residues within the epitope, the constrained conformation of this epitope, and a number of water-mediated interactions that stabilize the epitope. Our results now establish that the mobility of unusually long and bulged peptides bound to MHC-I is dependent on the sequence and hence the local structure of the bound epitope.

Although peptide determinants that are longer than the canonical 8/9-mer have been eluted from a number of class I molecules, the immunogenicity of such ligands in natural immune responses is largely unknown. Consequently, there are neither any data pertaining to the diversity of the T-cell repertoire nor significant insights into how a TcR can recognize such a complex. We have demonstrated that the HLA-B*3508^{LPEPLPQGQLTAY} complex is highly immunogenic, with 0.4–2% of the total CD8$^+$ CTL response directed against this bulged target (27). This high effector frequency, detectable in all HLA-B*3508 donors, opposes previous suggestions of large bulging targets impeding T-cell recognition (28). Strikingly, the T-cell repertoire against this epitope is highly restricted in all

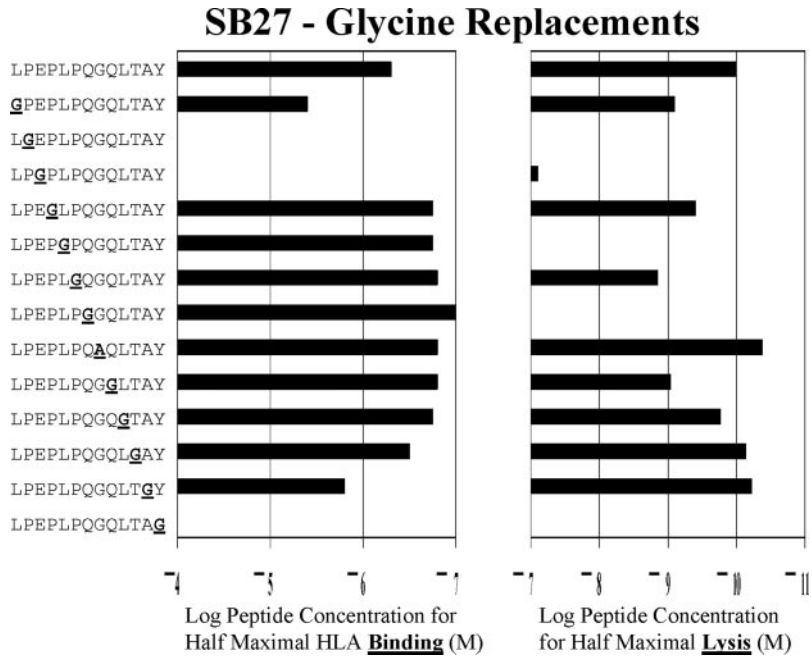

FIG. 4. **Impact of single amino acid substitutions within the LPEPLPQGQLTAY peptide on HLA-B*3508 binding and CTL recognition.** pMHC binding assays were conducted on a panel of 13-mer analog peptides into which single amino acid substitutions (Gly) were introduced. Each peptide was tested at a range of concentrations for its ability to stabilize HLA-B*3508 expression on the surface of the antigen-processing mutant T2 cell line. The concentration of each peptide required for half-maximum HLA-B*3508 stabilization was calculated and is shown. The CTL clone SB27 was also tested for recognition of the peptides. A range of peptide concentrations was used in these chromium release assays, and the concentration required for half-maximum lysis was calculated from these dose-response data and is shown.

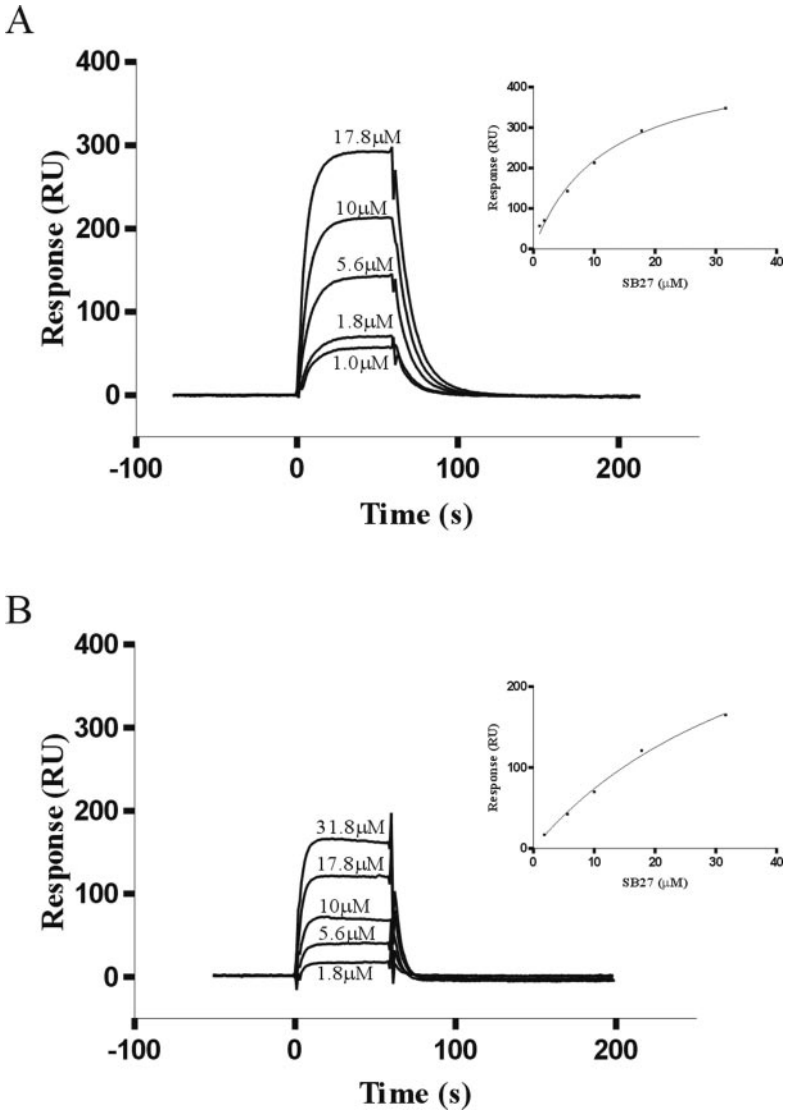

FIG. 5. **Analysis of the binding of the SB27 TcR to the HLA-B*3508 13-mer (*A*) and the HLA-B*3501 13-mer (*B*) by surface plasmon resonance.** SB27 at a range of concentrations was passed over immobilized HLA-B*3508 (*A*) or HLA-B*3501 (*B*), and the affinity and kinetic constants were determined. *Insets*, the equilibrium response *versus* concentration was plotted to give an equilibrium affinity of 9.9 μM (*A*) and 35.2 μM (*B*). *RU*, response units.

of the HLA-B*3508 donors we have examined, with the large majority of CTLs skewed toward the use of TRBV5-6, TRBV6-1, and TRAV19 chains. Conservation among Vβ chain sequences from different donors is less stringent compared with Vα chain sequences, although some of the Vβ genes display family and sequence homology. Thus, the TRAV19 chain, present in all donors, is identical in amino acid sequence, including those conserved residues encoded by N-region codons. The public TRAV19 α-chain is largely germ line-encoded, with only four nucleotides forming the N-region, which encodes a highly conserved Gly-Phe motif, which employs two different codons for the Gly residue. Nearly all of the CTL clones use the Jα TRAJ34 sequence, with variation from the TRAV19/TRAJ34 N-region Gly-Phe α-chain combination observed only at the V-J junction in 6 of 70 sequenced clones. Accordingly, the data imply that strong selection of particular Vα chain sequences is crucial for binding to the HLA-B*3508$^{\mathrm{LPEPLPQGQLTAY}}$ ligand.

Several questions arise concerning the strategy adopted by the restricted TcRs in recognizing such a bulged peptide·MHC complex. Is the interaction predominantly peptide-driven, akin to antibody/hapten interactions? To enable binding, does the TcR have unique properties, such as unusual CDR loop length that accommodates the complex? Does the TcR adopt a diagonal docking mode? Does the TcR effectively crumple the bulged region upon complexation? There appears to be nothing overtly unusual in the CDR3 sequences or loop length of these restricted TcRs. None of the other sequenced clones, including the representative SB27 TcR, possess particularly long CDR3 loops that might be anticipated to accommodate the bulged peptide. In addition, the CDR3 loops of the SB27 TcR are not glycine-rich, a feature that could have been predicted to be important in allowing plasticity of recognition of such an unusual epitope. Nevertheless, the slow on-rate for the SB27 TcR/HLA-B*3508$^{\mathrm{LPEPLPQGQLTAY}}$ interaction is consistent with a requirement for significant conformational adjustments of the TcR and/or the bulged region of the peptide for optimum binding.

Given that about one-third of the epitope is solvent-exposed, fine specificity analysis of SB27 CTL reactivity surprisingly revealed that only the N-terminal slope of the bulged epitope is critical for TcR recognition. Given the eccentric focus on the epitope by the SB27 TcR, it is somewhat puzzling how this TcR could engage with both the α1 and α2 helices of the HLA-B*3508 complex in a standard diagonal docking mode. Regardless, the SB27 TcR interacts with the HLA-B*3508$^{\mathrm{LPEPLPQGQLTAY}}$ complex with an affinity of 9.9 μM, which is well within the range observed for TcR/MHC-I interactions (46). Moreover, the long-lived half-life for this interaction indicates that, once the SB27 TcR is bound, a stable complex is formed.

Maintenance of MHC polymorphism reflects selection for induction of immunity toward diverse microbial ligands (47). Previously, it has been shown that polymorphic residues, although inaccessible to the TcR, can affect patterns of alloreactivity (17, 48–50) and TcR diversity (15, 16). Remarkably, the immunogenicity of the 13-mer epitope is controlled by a single amino acid polymorphism between HLA-B*3508 (Arg^{156}) and HLA-B*3501 (Leu^{156}) that is inaccessible to the TcR. The impact of this polymorphism results in a loss of interactions between the epitope and the heavy chain, although the conformation of the bound epitope *per se* is not significantly affected by the polymorphism. The impact of the polymorphism on TcR recognition appears to reside at a rigid body shift encompassing the ridge of the α2 helix of the MHC molecule. This effect on MHC structure, *viz.* a broadening of the antigen-binding cleft in HLA-B*3508, appears to be more favorable for TcR recognition of the HLA-B*3508·13-mer complex (K_d = 9.9 μM) compared with the HLA-B*3501·13-mer complex, which binds to SB27 with 4-fold reduced affinity (K_d = 35.2 μM). The latter falls below the range of TcR·pMHC complex affinities associated with priming of T-cell responses, being more comparable with the affinity of very weak agonists or antagonists (51). This finding and the lower thermostability of the HLA-B*3501·13-mer binary complex correlate well with the lack of immune response to this ligand in EBV-immune HLA-B*3501^{+} donors (51). Furthermore, the differential CTL recognition of the 13-mer complexed with HLA-B*3501 *versus* HLA-B*3508 implicates positions 145–152 as a contact region that interacts with the SB27 TcR as in a number of other TcR·pMHC complexes (22).

The binding preference of HLA-B35 allotypes for a P2-Pro is common among members of the HLA-B7 supertype (11, 52) and has been preserved in MHC-I molecules found in non-human primates (53) and rodents (54, 55). TAP translocation of cytosolic peptides into the endoplasmic reticulum is much less efficient when peptides contain proline residues near their N terminus (56–58), implying that only longer peptides that contain proline distal to the N terminus will be transported by TAP. Moreover, the endoplasmic reticulum peptide-trimming enzyme ERAAP (4, 59–61) is unable to cleave "*X*–Pro" bonds, so *X*-Pro-X_n peptides are likely to accumulate within the endoplasmic reticulum as longer precursors. Proline residues confer conformational constraints, often resulting in the introduction of a kink in the polypeptide chain (62, 63) that is likely to favor the looping out of relatively long peptides from the class I-binding cleft. It would therefore be advantageous if a proportion of class I molecules that exhibit specificity for Pro at P2 could also present peptides longer than the canonical 8/9-mer length. This property of MHC-I may be selected in the case of HLA-B35 based upon an ability to scavenge "indigestible" proline-containing peptide ligands that are sometimes longer than usual and that are unattractive to other class I types. The binding of longer peptides by class I allotypes such as HLA-B27 (24) and HLA-B35 may be facilitated because they can accommodate the looping conformation of long peptides principally ligated through the B- and F-pockets, whereas MHC class I molecules such as HLA-B8, HLA-B14, and H2-K^{b} also possess a central anchor residue in addition to these pockets. Our findings and those of others (26) demonstrate that HLA-B35 functions effectively in binding proline-containing epitopes of canonical and non-canonical length that induce T-cell responses. Notably, although the resulting TcR repertoire that can recognize such ligands appears to be constrained, there is sufficient plasticity to mount potent CTL responses that mediate viral immunity. The phenomenon of T-cell immunodominance and biased usage of particular V gene segments has been observed in the CTL response to a number of different viral infections (64), including EBV (65–67), measles (68), influenza (69, 70), and human immunodeficiency virus-1 (71). Our data suggest that public TcR usage can also reflect presentation of sterically demanding, bulged ligand structures and does not solely arise from the necessity to recognize featureless pMHC-I surfaces (72–74).

Acknowledgments—We thank A. Lesk for useful discussions and W. Macdonald, L. Ely, and H. Reid for critical reading of the manuscript. We thank the BioCARS staff at the Advanced Photon Source for assistance in data collection.

REFERENCES

1. Bastin, J., Rothbard, J., Davey, J., Jones, I., and Townsend, A. (1987) *J. Exp. Med.* **165,** 1508–1523
2. Gotch, F., Rothbard, J., Howland, K., Townsend, A., and McMichael, A. (1987) *Nature* **326,** 881–882
3. Deres, K., Beck, W., Faath, S., Jung, G., and Rammensee, H. G. (1993) *Cell. Immunol.* **151,** 158–167
4. Serwold, T., Gonzalez, F., Kim, J., Jacob, R., and Shastri, N. (2002) *Nature* **419,** 480–483

5. Falk, K., Rotzschke, O., Stevanovic, S., Jung, G., and Rammensee, H. G. (1991) *Nature* **351,** 290–296
6. Margulies, D., and McCluskey, J. (2003) in *Fundamental Immunology* (Paul, W., ed), 5th Ed., Lippincott Williams & Wilkins, Philadelphia
7. Guo, H. C., Madden, D. R., Silver, M. L., Jardetzky, T. S., Gorga, J. C., Strominger, J. L., and Wiley, D. C. (1993) *Proc. Natl. Acad. Sci. U. S. A.* **90,** 8053–8057
8. Rammensee, H. G., Falk, K., and Rotzschke, O. (1993) *Annu. Rev. Immunol.* **11,** 213–244
9. Falk, K., Rotzschke, O., Grahovac, B., Schendel, D., Stevanovic, S., Jung, G., and Rammensee, H. G. (1993) *Immunogenetics* **38,** 161–162
10. Steinle, A., Falk, K., Rotzschke, O., Gnau, V., Stevanovic, S., Jung, G., Schendel, D. J., and Rammensee, H. G. (1996) *Immunogenetics* **43,** 105–107
11. Sidney, J., del Guercio, M. F., Southwood, S., Engelhard, V. H., Appella, E., Rammensee, H. G., Falk, K., Rotzschke, O., Takiguchi, M., Kubo, R. T., Grey, H. M., and Sette, A. (1995) *J. Immunol.* **154,** 247–259
12. Takamiya, Y., Schonbach, C., Nokihara, K., Yamaguchi, M., Ferrone, S., Kano, K., Egawa, K., and Takiguchi, M. (1994) *Int. Immunol.* **6,** 255–261
13. Schonbach, C., Ibe, M., Shiga, H., Takamiya, Y., Miwa, K., Nokihara, K., and Takiguchi, M. (1995) *J. Immunol.* **154,** 5951–5958
14. Maryanski, J. L., Casanova, J. L., Falk, K., Gournier, H., Jaulin, C., Kourilsky, P., Lemonnier, F. A., Luthy, R., Rammensee, H. G., Rotzschke, O., Servis, C., and Lopez, J. A. (1997) *Hum. Immunol.* **54,** 117–128
15. Dyall, R., Messaoudi, I., Janetzki, S., and Nikolic-Zugic, J. (2000) *J. Immunol.* **164,** 1695–1698
16. Messaoudi, I., Patino, J. A., Dyall, R., LeMaoult, J., and Nikolich-Zugich, J. (2002) *Science* **298,** 1797–1800
17. Macdonald, W. A., Purcell, A. W., Mifsud, N. A., Ely, L. K., Williams, D. S., Chang, L., Gorman, J. J., Clements, C. S., Kjer-Nielsen, L., Koelle, D. M., Burrows, S. R., Tait, B. D., Holdsworth, R., Brooks, A. G., Lovrecz, G. O., Lu, L., Rossjohn, J., and McCluskey, J. (2003) *J. Exp. Med.* **198,** 679–691
18. Villadangos, J. A., Galocha, B., Lopez, D., Calvo, V., and Lopez de Castro, J. A. (1992) *J. Immunol.* **149,** 505–510
19. Lopez, D., Garcia-Hoyo, R., and Lopez de Castro, J. A. (1994) *J. Immunol.* **152,** 5557–5571
20. Fremont, D. H., Matsumura, M., Stura, E. A., Peterson, P. A., and Wilson, I. A. (1992) *Science* **257,** 919–927
21. Madden, D. R., Garboczi, D. N., and Wiley, D. C. (1993) *Cell* **75,** 693–708
22. Zhang, W., Young, A. C., Imarai, M., Nathenson, S. G., and Sacchettini, J. C. (1992) *Proc. Natl. Acad. Sci. U. S. A.* **89,** 8403–8407
23. Chen, Y., Sidney, J., Southwood, S., Cox, A. L., Sakaguchi, K., Henderson, R. A., Appella, E., Hunt, D. F., Sette, A., and Engelhard, V. H. (1994) *J. Immunol.* **152,** 2874–2881
24. Urban, R. G., Chicz, R. M., Lane, W. S., Strominger, J. L., Rehm, A., Kenter, M. J., UytdeHaag, F. G., Ploegh, H., Uchanska-Ziegler, B., and Ziegler, A. (1994) *Proc. Natl. Acad. Sci. U. S. A.* **91,** 1534–1538
25. Speir, J. A., Stevens, J., Joly, E., Butcher, G. W., and Wilson, I. A. (2001) *Immunity* **14,** 81–92
26. Probst-Kepper, M., Stroobant, V., Kridel, R., Gaugler, B., Landry, C., Brasseur, F., Cosyns, J. P., Weynand, B., Boon, T., and Van Den Eynde, B. J. (2001) *J. Exp. Med.* **193,** 1189–1198
27. Green, K. J., Miles, J. J., Tellam, J., van Zuylen, W. J., Connolly, G., and Burrows, S. R. (2004) *Eur. J. Immunol.* **34,** 2510–2519
28. Guo, H. C., Jardetzky, T. S., Garrett, T. P., Lane, W. S., Strominger, J. L., and Wiley, D. C. (1992) *Nature* **360,** 364–366
29. Horig, H., Young, A. C., Papadopoulos, N. J., DiLorenzo, T. P., and Nathenson, S. G. (1999) *J. Immunol.* **163,** 4434–4441
30. Stryhn, A., Pedersen, L. O., Holm, A., and Buus, S. (2000) *Eur. J. Immunol.* **30,** 3089–3099
31. Wilson, I. A., and Fremont, D. H. (1993) *Semin. Immunol.* **5,** 75–80
32. Glithero, A., Tormo, J., Haurum, J. S., Arsequell, G., Valencia, G., Edwards, J., Springer, S., Townsend, A., Pao, Y.-L., and Wormald, M. (1999) *Immunity* **10,** 63–74
33. Zavala-Ruiz, Z., Strug, I., Walker, B. D., Norris, P. J., and Stern, L. J. (2004) *Proc. Natl. Acad. Sci. U. S. A.* **101,** 13279–13284
34. Salter, R. D., and Cresswell, P. (1986) *EMBO J.* **5,** 943–949
35. Khanna, R., Silins, S. L., Weng, Z., Gatchell, D., Burrows, S. R., and Cooper, L. (1999) *Eur. J. Immunol.* **29,** 1587–1597
36. Panzara, M. A., Gussoni, E., Steinman, L., and Oksenberg, J. R. (1992) *BioTechniques* **12,** 728–735
37. Lefranc, M. P. (2001) *Nucleic Acids Res.* **29,** 207–209
38. Macdonald, W., Williams, D. S., Clements, C. S., Gorman, J. J., Kjer-Nielsen, L., Brooks, A. G., McCluskey, J., Rossjohn, J., and Purcell, A. W. (2002) *FEBS Lett.* **527,** 27–32
39. Rossmann, M. G., and van Beek, C. G. (1999) *Acta Crystallogr. Sect. D Biol. Crystallogr.* **55,** 1631–1640
40. Jones, T. A., Zou, J. Y., Cowan, S. W., and Kjeldgaard. (1991) *Acta Crystallogr. Sect. A* **47,** 110–119
41. Brunger, A. T., Adams, P. D., Clore, G. M., DeLano, W. L., Gros, P., Grosse-Kunstleve, R. W., Jiang, J. S., Kuszewski, J., Nilges, M., Pannu, N. S., Read, R. J., Rice, L. M., Simonson, T., and Warren, G. L. (1998) *Acta Crystallogr. Sect. D Biol. Crystallogr.* **54,** 905–921
42. Borg, N. A., Ely, L. K., Beddoe, T., Macdonald, W. A., Reid, H. H., Clements, C. S., Purcell, A. W., Kjer-Nielsen, L., Miles, J. J., Burrows, S. R., McCluskey, J., and Rossjohn, J. (2005) *Nat. Immunol.* **6,** 171–180
43. Parham, P., Barnstable, C. J., and Bodmer, W. F. (1979) *J. Immunol.* **123,** 342–349
44. Menssen, R., Orth, P., Ziegler, A., and Saenger, W. (1999) *J. Mol. Biol.* **285,** 645–653
45. Smith, K. J., Reid, S. W., Stuart, D. I., McMichael, A. J., Jones, E. Y., and Bell, J. I. (1996) *Immunity* **4,** 203–213
46. van der Merwe, P. A., and Davis, S. J. (2003) *Annu. Rev. Immunol.* **21,** 659–684
47. Parham, P., and Ohta, T. (1996) *Science* **272,** 67–74
48. Lombardi, G., Matsui, M., Moots, R., Aichinger, G., Sidhu, S., Batchelor, R., Frelinger, J., and Lechler, R. (1991) *Immunogenetics* **34,** 149–156
49. Bluestone, J. A., Langlet, C., Geier, S. S., Nathenson, S. G., Foo, M., and Schmitt-Verhulst, A. M. (1986) *J. Immunol.* **137,** 1244–1250
50. Murray, R., Hutchison, C. A., III, and Frelinger, J. A. (1988) *Proc. Natl. Acad. Sci. U. S. A.* **85,** 3535–3539
51. Rudolph, M. G., and Wilson, I. A. (2002) *Curr. Opin. Immunol.* **14,** 52–65
52. Sette, A., and Sidney, J. (1999) *Immunogenetics* **50,** 201–212
53. Bertoni, R., Sette, A., Sidney, J., Guidotti, L. G., Shapiro, M., Purcell, R., and Chisari, F. V. (1998) *J. Immunol.* **161,** 4447–4455
54. Sette, A., Sidney, J., Livingston, B. D., Dzuris, J. L., Crimi, C., Walker, C. M., Southwood, S., Collins, E. J., and Hughes, A. L. (2003) *Immunogenetics* **54,** 830–841
55. Norda, M., Falk, K., Rotzschke, O., Stevanovic, S., Jung, G., and Rammensee, H. G. (1993) *J. Immunother.* **14,** 144–149
56. Heemels, M. T., and Ploegh, H. (1995) *Annu. Rev. Biochem.* **64,** 463–491
57. Androlewicz, M. J., and Cresswell, P. (1996) *Immunity* **5,** 1–5
58. Uebel, S., and Tampe, R. (1999) *Curr. Opin. Immunol.* **11,** 203–208
59. Serwold, T., Gaw, S., and Shastri, N. (2001) *Nat. Immunol.* **2,** 644–651
60. Saric, T., Chang, S. C., Hattori, A., York, I. A., Markant, S., Rock, K. L., Tsujimoto, M., and Goldberg, A. L. (2002) *Nat. Immunol.* **3,** 1169–1176
61. York, I. A., Chang, S. C., Saric, T., Keys, J. A., Favreau, J. M., Goldberg, A. L., and Rock, K. L. (2002) *Nat. Immunol.* **3,** 1177–1184
62. Yaron, A., and Naider, F. (1993) *Crit. Rev. Biochem. Mol. Biol.* **28,** 31–81
63. Vanhoof, G., Goossens, F., De Meester, I., Hendriks, D., and Scharpe, S. (1995) *FASEB J.* **9,** 736–744
64. Callan, M. F., and McMichael, A. J. (1999) *Springer Semin. Immunopathol.* **21,** 37–54
65. Argaet, V. P., Schmidt, C. W., Burrows, S. R., Silins, S. L., Kurilla, M. G., Doolan, D. L., Suhrbier, A., Moss, D. J., Kieff, E., Sculley, T. B., and Misko, I. S. (1994) *J. Exp. Med.* **180,** 2335–2340
66. Callan, M. F., Annels, N., Steven, N., Tan, L., Wilson, J., McMichael, A. J., and Rickinson, A. B. (1998) *Eur. J. Immunol.* **28,** 4382–4390
67. Callan, M. F., Fazou, C., Yang, H., Rostron, T., Poon, K., Hatton, C., and McMichael, A. J. (2000) *J. Clin. Investig.* **106,** 1251–1261
68. Mongkolsapaya, J., Jaye, A., Callan, M. F., Magnusen, A. F., McMichael, A. J., and Whittle, H. C. (1999) *J. Virol.* **73,** 67–71
69. Callan, M. F., Gillespie, G. M., Reyburn, H. T., Moss, P. A., Bell, J. I., and McMichael, A. J. (1995) *Ann. N. Y. Acad. Sci.* **756,** 94–95
70. Kedzierska, K., Turner, S. J., and Doherty, P. C. (2004) *Proc. Natl. Acad. Sci. U. S. A.* **101,** 4942–4947
71. Wilson, J. D., Ogg, G. S., Allen, R. L., Goulder, P. J., Kelleher, A., Sewell, A. K., O'Callaghan, C. A., Rowland-Jones, S. L., Callan, M. F., and McMichael, A. J. (1998) *J. Exp. Med.* **188,** 785–790
72. Kjer-Nielsen, L., Clements, C. S., Purcell, A. W., Brooks, A. G., Whisstock, J. C., Burrows, S. R., McCluskey, J., and Rossjohn, J. (2003) *Immunity* **18,** 53–64
73. Stewart-Jones, G. B., McMichael, A. J., Bell, J. I., Stuart, D. I., and Jones, E. Y. (2003) *Nat. Immunol.* **4,** 657–663
74. Davis, M. M. (2003) *Nat. Immunol.* **4,** 649–650
75. Boulter, J. M., Glick, M., Todorov, P. T., Baston, E., Sami, M., Rizkallah, P., and Jakobsen, B. K. (2003) *Protein Eng.* **16,** 707–711
76. Garboczi, D. N., Utz, U., Ghosh, P., Seth, A., Kim, J., VanTienhoven, E. A., Biddison, W. E., and Wiley, D. C. (1996) *J. Immunol.* **157,** 5403–5410

SB27 - Glycine Replacements

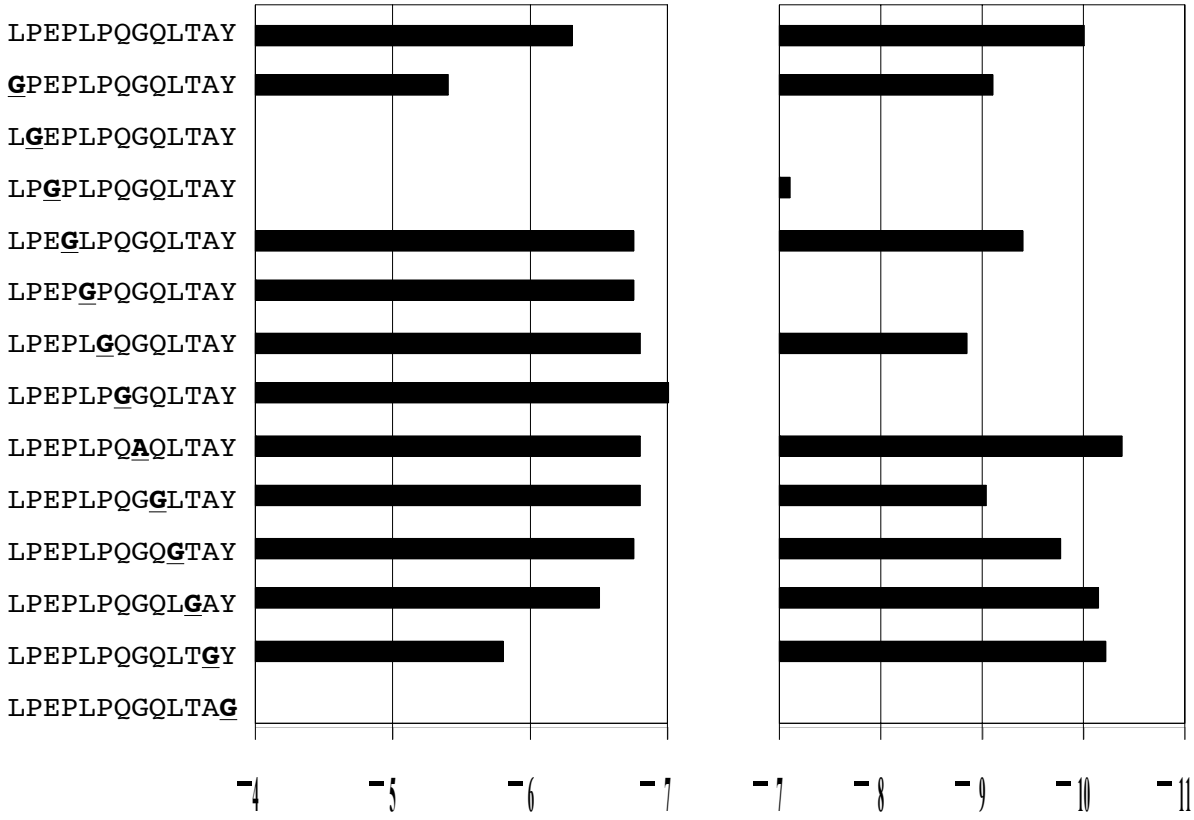

High Resolution Structures of Highly Bulged Viral Epitopes Bound to Major Histocompatibility Complex Class I: IMPLICATIONS FOR T-CELL RECEPTOR ENGAGEMENT AND T-CELL IMMUNODOMINANCE

Fleur E. Tynan, Natalie A. Borg, John J. Miles, Travis Beddoe, Diah El-Hassen, Sharon L. Silins, Wendy J. M. van Zuylen, Anthony W. Purcell, Lars Kjer-Nielsen, James McCluskey, Scott R. Burrows and Jamie Rossjohn

J. Biol. Chem. 2005, 280:23900-23909.
doi: 10.1074/jbc.M503060200 originally published online April 22, 2005
